Supporting Information: Multielectron, Cation and Anion Redox in Lithium-Rich Iron Sulfide Cathodes

Charles J. Hansen,[†] Joshua J. Zak,[†] Andrew J. Martinolich,[†] Jesse S. Ko,[‡] Nicholas H. Bashian,[¶] Farnaz Kaboudvand,[§] Anton Van der Ven,[§] Brent C. Melot,[¶] Johanna Nelson Weker,[‡] and Kimberly A. See[*,†]

†*Division of Chemistry and Chemical Engineering, California Institute of Technology, Pasadena, California 91125, United States*

‡*Stanford Synchrotron Radiation Lightsource, SLAC National Accelerator Laboratory, Menlo Park, California 94025, United States*

¶*Department of Chemistry, University of Southern California, Los Angeles, California 90089, United States*

§*Materials Department, University of California, Santa Barbara, California 93106, United States*

E-mail: ksee@caltech.edu

Experimental Details

Na_2S was prepared from stoichiometric Na (Acros Organics, rod, 99.8%, mechanically cleaned prior to use) and S (see main text) in separate alumina crucibles (Almath) in an evacuated silica ampoule. The reactants were heated at 1 °C min^{-1} to 300 °C for 48 h and cooled ambiently to room temperature. The ground product was a fine powder of a slightly tan-color. The product was determined to be phase pure by XRD.

The *operando* electrochemical cell comprised of a 1.2" (I.D.) stainless steel Swagelok union with a thin sheet of plastic wrapped around the interior of the cell to prevent the electrodes from shorting. The stack inside the cell included the Be window and current collector, the free-standing electrode (cathode), a glass-fiber separator (Whatman, GF/D), a Li foil anode, a spacer, a spring, and a stainless steel plunger that served as the other current collector. The cell was flooded with LP100 electrolyte and sealed around the plunger with PTFE ferrules. The cell was placed on the diffractometer stage such that the X-rays would directly access the cathode after penetrating the Be window. A VMP3 mutli-channel potentiostat (Bio-Logic) was used to perform the electrochemical experiments.

Supplemental Tables and Figures

Tables S1-S2 include potential impurities that appear absent from the high-resolution powder X-ray diffraction (XRD) data for Li_2FeS_2 and $LiNaFeS_2$, respectively. Note that in the tables the variables x, y, z, and *n* may take on any value corresponding to reported phases in the Inorganic Crystal Structure Database including 0 (e.g. LiOH is a valid compound under "$LiOH \cdot n\ H_2O$").

Table S1: List of potential impurities not found in Li_2FeS_2 based on the 11-BM XRD data.

precursors	other sulfides	reaction with tube	air exposure
Fe	FeS	graphite	$LiOH \cdot n\ H_2O$
pyrite-FeS_2	Fe_7S_8	LiC_6	$Li_xFe_yO_z \cdot n\ H_2O$
	Fe_3S_4	$Fe_xSi_yO_z$	$Li_xFe_y(SO_4)_z \cdot n\ H_2O$
	marcasite-FeS_2		
	computed Li_2FeS_2 polymorphs		

Table S2: List of potential impurities not found in $LiNaFeS_2$ based on the 11-BM XRD data.

precursors	other sulfides	reaction with tube	air exposure
Fe	FeS	$Fe_xSi_yO_z$	Fe_xO_y
S_8	Fe_7S_8	$Li_xFe_yO_z$	$Li_xFe_y(SO_4)_z$
Li_2S	Fe_3S_4	$Na_xFe_yO_z$	$LiOH \cdot n\ H_2O$
Na_2S	marcasite-FeS_2		$NaOH \cdot n\ H_2O$
Na	pyrite-FeS_2		$Li_xFe_y(SO_4)_z \cdot n\ H_2O$
	$Na_xFe_yS_z$		$Na_xFe_y(SO_4)_z \cdot n\ H_2O$

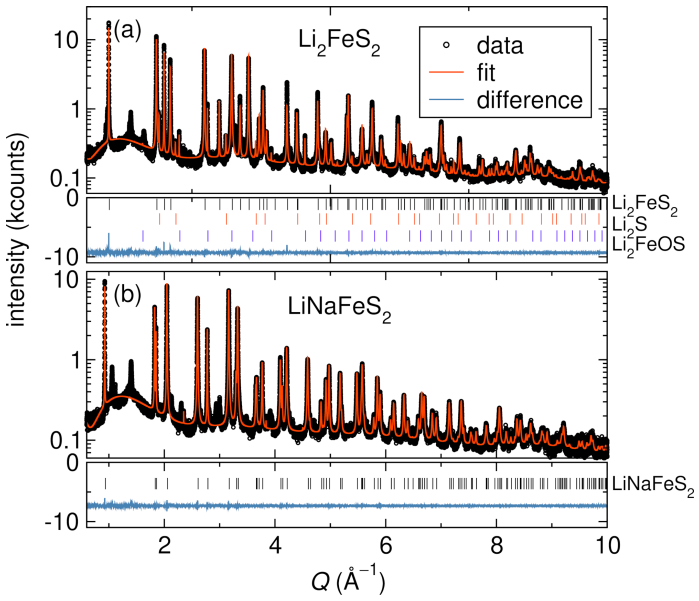

Figure S1: Synchrotron X-ray diffraction at 11-bm of (a) Li_2FeS_2 and (b) $LiNaFeS_2$. The Rietveld refinement and resulting difference trace are shown for each material. The refinement in (a) is a three-phase fit to Li_2FeS_2, < 2 wt% Li_2S and < 3 wt% Li_2FeOS, while the refinement in (b) is a single $LiNaFeS_2$ phase. The tick marks identify the locations of the Bragg reflections of the phases included in each fit.

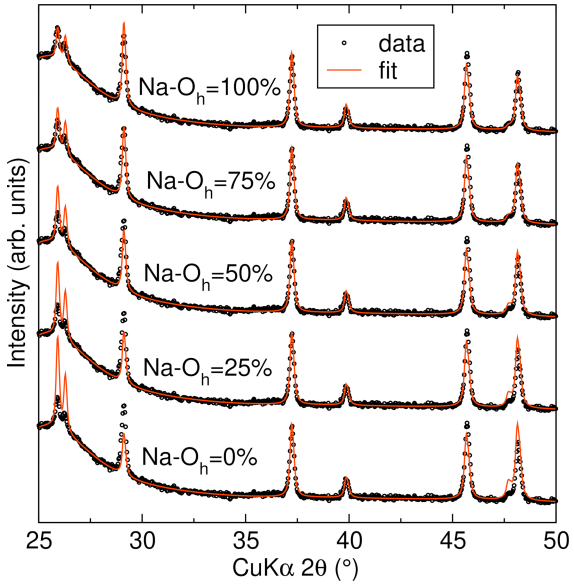

Figure S2: XRD data and Rietveld refinement of $LiNaFeS_2$ with varying degrees of site mixing. The rise in the background over *ca.* 25°-35° (2θ) is due to the polyimide tape covering the sample and the grease fixing the sample to the glass slide. The best fit is achieved at 100% of the Na sitting in the O_h site. A similar trend is observed in Li_2FeS_2, in that the relative intensities of different reflections are not maintained as Fe is mixed onto the octahedral site.

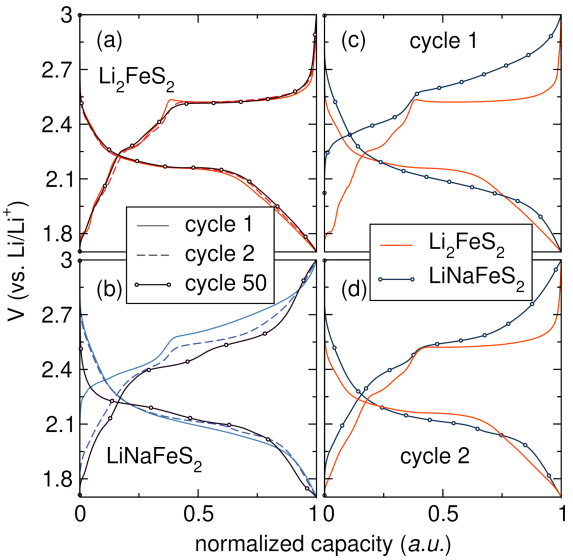

Figure S3: Comparison of galvanostatic profile of cycles 1, 2, and 50 for (a) Li_2FeS_2 and (b) $LiNaFeS_2$ normalized to the maximum capacity in the given charge or discharge half-cycle. Direct comparison of Li_2FeS_2 and $LiNaFeS_2$ discharge/charge profiles in (c) cycle 1 and (d) cycle 2.

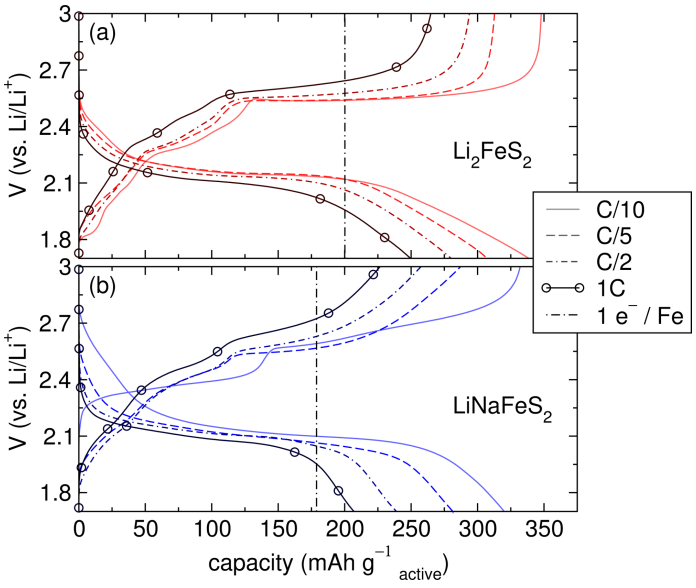

Figure S4: Galvanostatic cycling of (a) Li_2FeS_2 and (b) $LiNaFeS_2$ at various rates (indicated). The profiles shown are the first cycle of five at the specified rate, moving from the slowest to fastest (i.e. *C*/10) to 1 *C*, in accordance with the data shown in the main text.

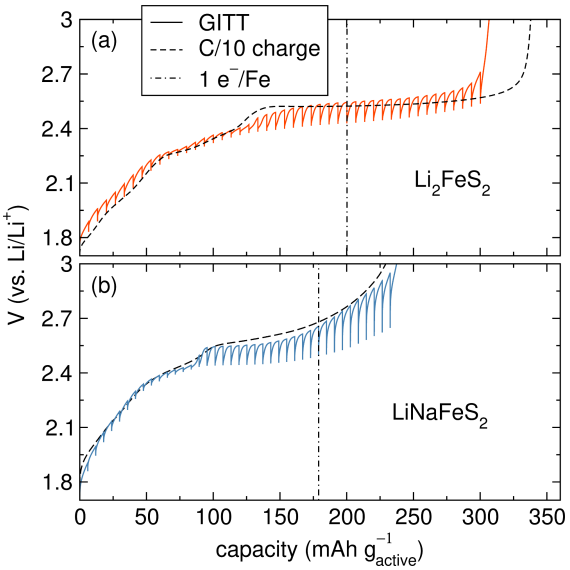

Figure S5: GITT data on the second charge and representative galvanostatic charge profile (for reference) of Li_2FeS_2 (a) and $LiNaFeS_2$ (b) with a Li metal anode, LP100 electrolyte, and 50 wt% (active material) drop-cast electrodes. The current in the GITT experiments was $C/10$ based on one electron per formula unit for 20 min seprated by 4 h rest periods.

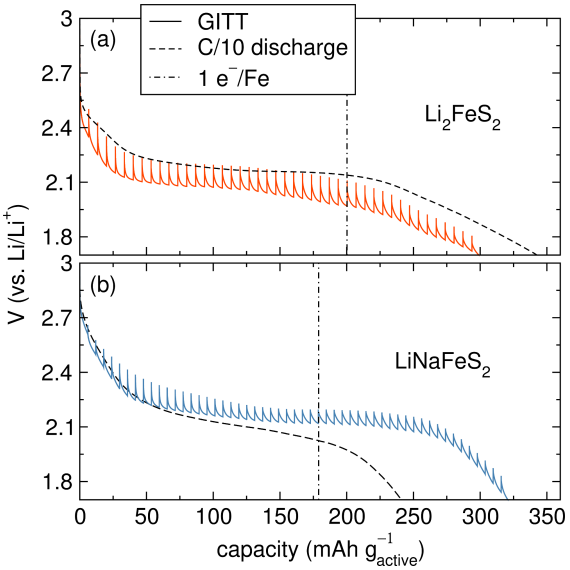

Figure S6: GITT data on the first discharge and representative galvanostatic charge profile (for reference) of (a) Li_2FeS_2 and (b) $LiNaFeS_2$ with the same experimental details as Figure S5.

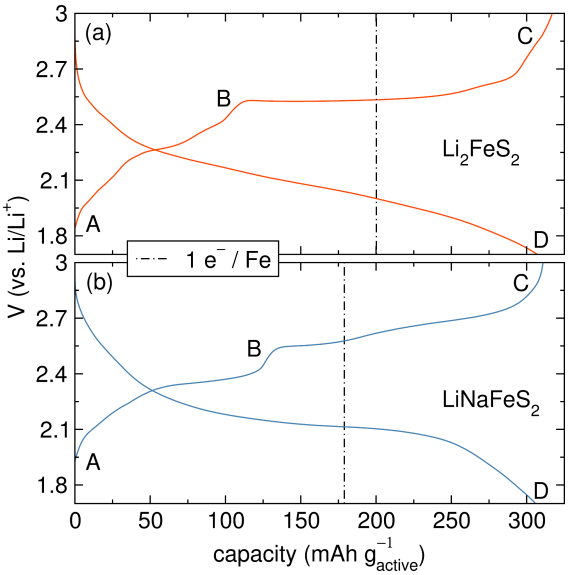

Figure S7: Representative electrochemistry and cutoff points for S K-edge XAS samples for Li_2FeS_2 (a) and $LiNaFeS_2$ (b). Cutoffs A-D are the pristine material, charged to 2.5 V, fully charged to 3 V, and fully charged then fully discharged to 1.7 V, respectively. The cells were charged at *C*/10 based on one electron per formula unit with a Li metal anode, LP100 electrolyte, and 60 wt% (active material) free-standing electrodes in 1/2" Swagelok cells.

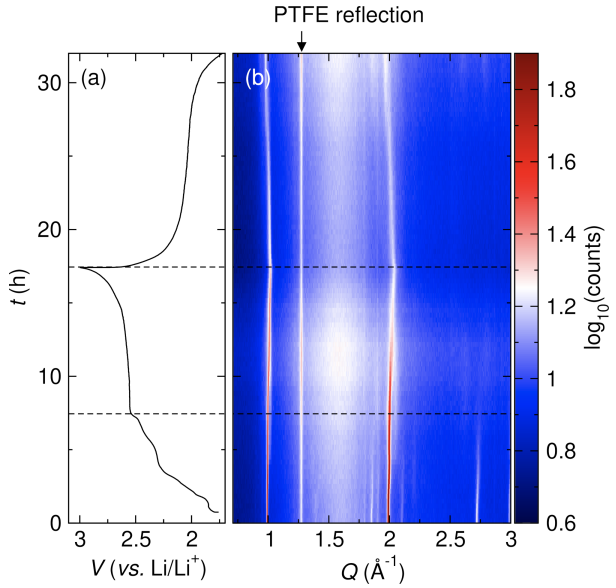

Figure S8: (a) Galvanostatic charge and discharge curve of Li_2FeS_2 obtained during *operando* XRD and (b) the corresponding diffraction patterns. The capacity obtained on charge in this cell was 334 mAh g^{-1} (or *ca.* 1.7 electrons), consistent with the other cell geometries in this work. The cells were allowed to rest at open circuit for the first two scans (thus the voltage is constant for the first *ca.* 1 h).

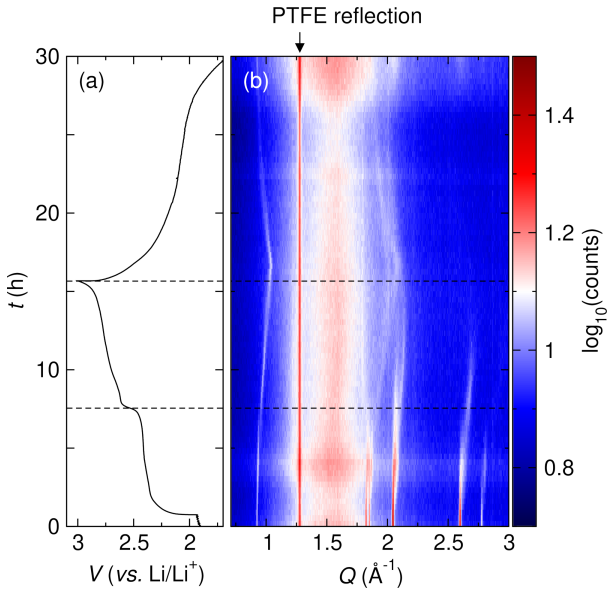

Figure S9: (a) Galvanostatic charge and discharge curve of $LiNaFeS_2$ obtained during *operando* XRD and (b) the corresponding diffraction patterns. The capacity obtained on charge in this cell was 268 mAh g^{-1} (or *ca.* 1.5 electrons), consistent with the other cell geometries in this work. The cells were allowed to rest at open circuit for the first two scans (thus the voltage is constant for the first *ca.* 1 h).

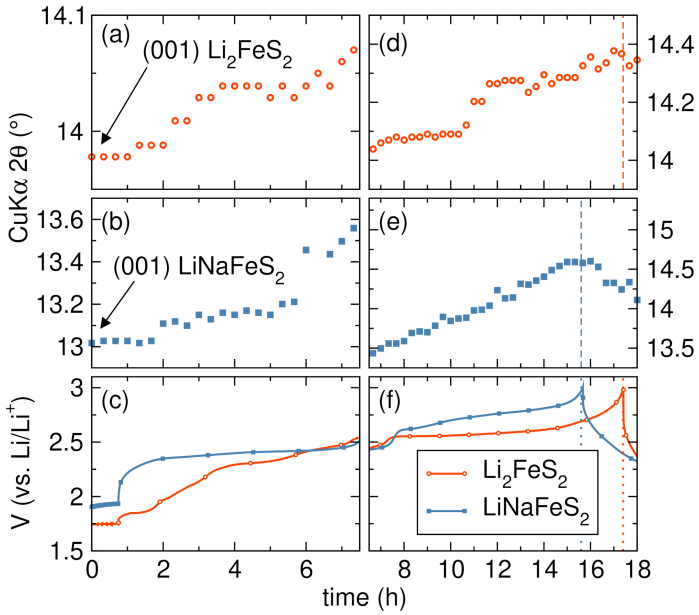

Figure S10: The position of the Bragg peak extracted from the *operando* XRD data that begins as the (001) reflection in (a) Li_2FeS_2 and (b) $LiNaFeS_2$ as a function of oxidation along with (c) the corresponding electrochemistry up to 2.5 V. The position of the Bragg peak that begins as the (001) reflection in (d) Li_2FeS_2 and (e) $LiNaFeS_2$ as a function of oxidation along with (f) the corresponding electrochemistry up to 3 V.

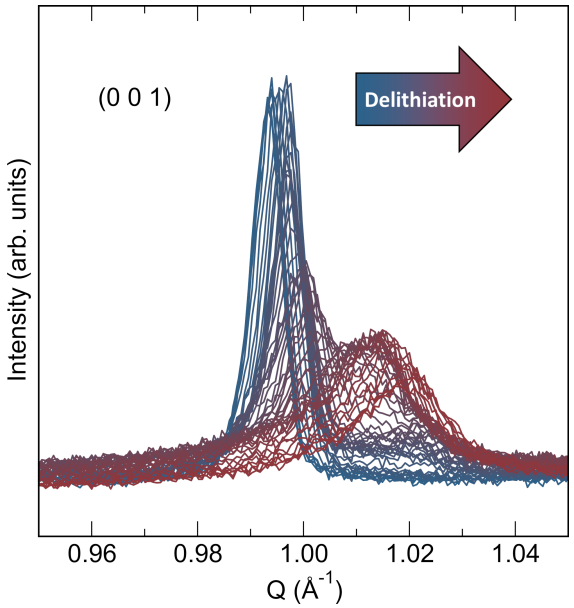

Figure S11: *Operando* XRD during delithation of Li_2FeS_2 focused on the (001) reflection. The reflection shifts systematically and is then replaced by a new reflection at higher Q.

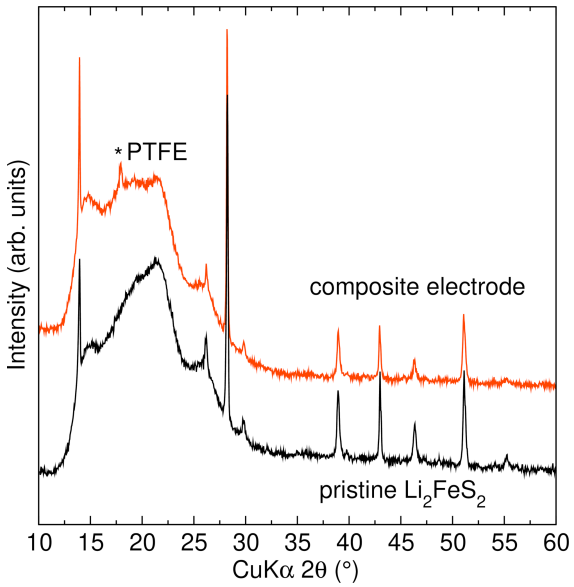

Figure S12: XRD data of pristine Li_2FeS_2 and a 60 wt% Li_2FeS_2 free-standing composite electrode. The * at *ca.* 17° denotes a reflection due to the PTFE binder in the electrode. The rise in the background over *ca.* 12°-30° (2θ) is due to the polyimide tape covering the sample and the grease fixing the sample to the glass slide.

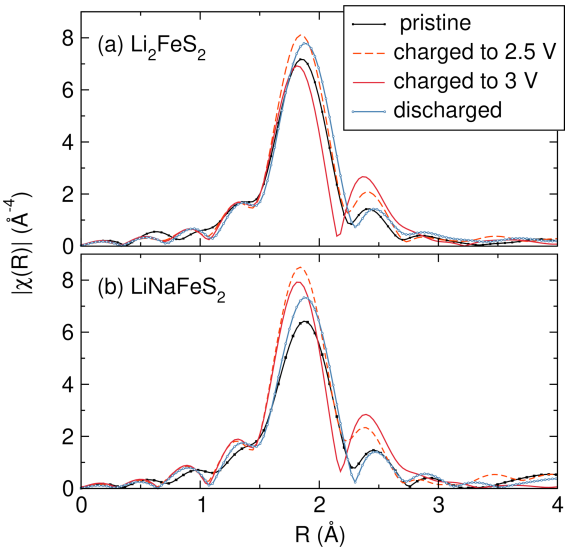

Figure S13: k^3-Weighted FT-spectra of the Fe K-edge EXAFS of (a) Li_2FeS_2 and (b) $LiNaFeS_2$ at various states of charge.

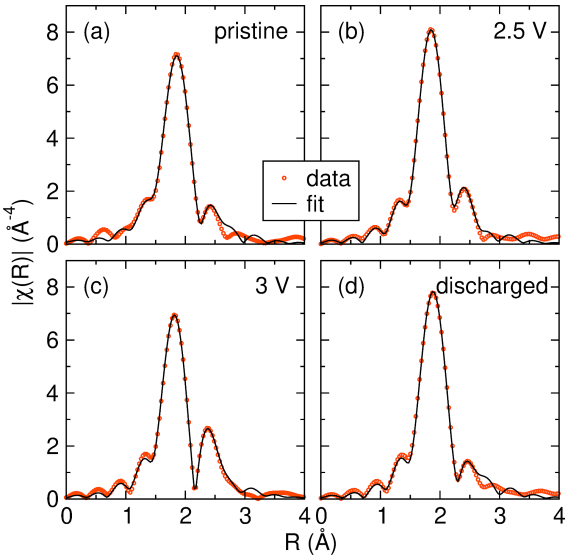

Figure S14: k^3-Weighted FT-spectra of the Fe K-edge EXAFS of Li_2FeS_2 of (a) pristine, (b) charged to 2.5 V, (c) charged to 3 V, and (d) discharged samples with corresponding fits to the first and second coordination shells.

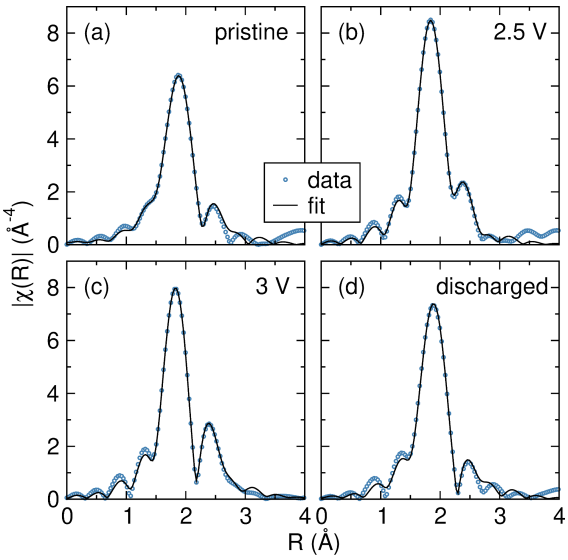

Figure S15: k^3-Weighted FT-spectra of the Fe K-edge EXAFS of $LiNaFeS_2$ of (a) pristine, (b) charged to 2.5 V, (c) charged to 3 V, and (d) discharged samples with corresponding fits to the first and second coordination shells.

Table S3: Coordination numbers of the first shell (N_1) and second shell (N_2) with associated average bond lengths obtained from fitting the Fe K-edge EXAFS data.

			Li_2FeS_2		
	N_1	Fe-S (Å)	N_2	Fe-Fe (Å)	σ^2
pristine	3.7 ± 0.2	2.30 ± 0.01	0.8 ± 0.2	2.71 ± 0.02	0.006
charged to 2.5 V	2.9 ± 0.1	2.26 ± 0.01	0.4 ± 0.1	2.76 ± 0.01	0.003
charged to 3 V	2.6 ± 0.1	2.25 ± 0.01	0.9 ± 0.1	2.69 ± 0.01	0.004
discharged to 1.7 V	3.1 ± 0.3	2.31 ± 0.01	0.7 ± 0.1	2.70 ± 0.02	0.004

			$LiNaFeS_2$		
	N_1	Fe-S (Å)	N_2	Fe-Fe (Å)	σ^2
pristine	4.0*	2.33 ± 0.01	0.9 ± 0.2	2.78 ± 0.02	0.008
charged to 2.5 V	2.9 ± 0.1	2.25 ± 0.01	0.4 ± 0.1	2.77 ± 0.01	0.003
charged to 3 V	2.8 ± 0.1	2.25 ± 0.01	0.8 ± 0.1	2.70 ± 0.91	0.003
discharged to 1.7 V	3.3 ± 0.3	2.32 ± 0.01	0.5 ± 0.2	2.75 ± 0.03	0.005

*used as standard, coordination number set to 4.0